ResearchGate

See discussions, stats, and author profiles for this publication at: https://www.researchgate.net/publication/281833266

Modeling of Washing Circuits in Mining – A Networked System Approach

CONFERENCE PAPER · JUNE 2015

DOI: 10.13140/RG.2.1.1744.1767

READS

22

2 AUTHORS:

Tri Tran

Nanyang Technological University, Cambri…

48 PUBLICATIONS **92** CITATIONS

SEE PROFILE

Quang Ha

University of Technology Sydney

213 PUBLICATIONS **2,010** CITATIONS

SEE PROFILE

All in-text references underlined in blue are linked to publications on ResearchGate, letting you access and read them immediately.

Available from: Tri Tran
Retrieved on: 18 March 2016

Modeling of Washing Circuits in Mining - A Networked System Approach

Tri Tran and Q. P. Ha

***Abstract*— The models of two process system networks in an alumina refinery are developed in this paper. These models have been used in the numerical simulations in previous work. They are the washing circuits widely used in the mineral processing plants. The process modeling here is to derive a state space model for the multi-variable feedback control design purpose. The complex process system is modelled as an interconnected system having a mixed connection configuration. The interactions between equipment and sub-processes via the material flows within an unit operation are modelled as interactive variables of subsystems under the auspices of interconnected system formulation.**

I. Introduction

In the production of alumina from the bauxite ores, the Bayer cycle is recognised as a unique processing technology. A block diagram of the Bayer cycle is illustrated in Figure 1 below, whereby there are four main departments, namely Predesilication and Digestion, Clarification and Washing, Precipitation and Evaporation.

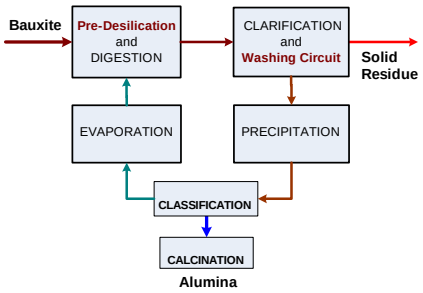

Fig. 1. The Bayer cycle of bauxite refining.

The production basically dilutes the red bauxite ore in certain forms, most likely is the solid Gibbsite - Trihydrate, Boehmite - Monohydrate ($Al_2O_3.H_2O$) and Kaolinite ($Al_2O_3.2SiO_2.2H_2O$), together with some impurities, such as, Silica (SiO_2), Iron Oxide (Fe_2O_3) and Titania (TiO_2), to obtain the soluble $NaAlO_2$ and the solid desilication product $3Na_2O.3Al_2O3.5SiO_2.5H_2O$ (in the Digestion stage). It is then going through a series of Clarification and Precipitation stages, then subsequently through the Classification and Calcination stages to become the final product of white alumina powder (Al_2O_3). Waters from the residue liquors are recovered by the Evaporators and fed back to the Digestion stage. The residue solids are washed to eliminate all toxic chemicals before being deposited into tight ponds. Some references for the alumina refining process can be found in [1], [2], [3], [4], [5], [6], [7], [8]. A typical counter-current Washing Circuit and a circulated Pre-desilication are considered in this paper.

This work was partially supported by the National Research Foundation (NRF) of Singapore under its Campus for Research Excellence And Technological Enterprise (CREATE) programme, and the Cambridge Centre for Advanced Research in Energy Efficiency in Singapore (Cambridge CARES).

Tri Tran is currently with Cambridge CARES, Nanyang Technological University, Singapore. Email: tctran@ieee.org

Q. P. Ha is with Faculty of Engineering and Information Technology, University of Technology, Sydney, Australia. Email: Quang.Ha@uts.edu.au

II. The Counter-Current Washing Circuit

The counter-current washing technology is widespread used in the mineral processing industry. The process flow diagram of a typical washing circuit is given in Figure 2. In an alumina refinery, the washing circuit recovers caustic soda from the residues of the upstream thickeners and clarifiers. Three residue washers are normally in operation. The inlet slurry is fed into the first washing stage while fresh condensates (water) are added to the final stage. The level of liquor on the top and the level of residue solids in the bottom of each washing tank will be continuously measured and controlled. Each washing stage (a tank) will have an underflow and overflow pump (e.g. P-11 and P-12, respectively, of the first tank in Figure 2).

The main inlets of a washing tank will be from the upstream underflow and downstream overflow. The mixing of underflow and overflow streams will occur in a mixer prior to feeding into each tank. Flocculants are added after the slurry is mixed to enhance the settling conditions. The settled residue which has lower levels of caustic is raked to the tank perimeter where it is removed and pumped to the next downstream stage. The overflow liquor which has higher levels of caustic is pumped to the next upstream tank. The caustic content is thus reduced as residues move down the washing circuit. The underflow rates are linearly proportional to the residue levels while the overflow rates are proportional to the liquor levels.

A washing stage is represented by a subsystem state space model in this control modeling approach. Three controlled variables (plant outputs) of each subsystems correspond to the residue level, liquor level and slurry density. The manipulated variables of the first tank are the feeding slurry and flocculant flow rates, of the second tank is the flocculant flow rate, and of the third tank are the condensate and flocculant flow rates. A modular control strategy has been applied to this washing circuit instead of a plant wide strategy, wherein

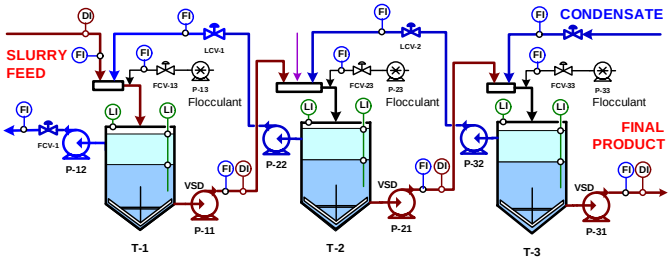

Fig. 2. A typical counter-current Washing Circuit.

the regulations of the underflow and overflow pumps depend only on the liquor and residue levels of the same stage.

1) State Space Model: The continuous-time state space models of the interaction-oriented format presented by [9] are given here. In the interaction-oriented models, the coupling vectors (or interaction vectors) between subsystems are explicitly articulated as input and output vectors. Only non feed-through systems are considered in this paper. The system models are depicted by the block diagram in Figure 3. The state space model of the large-scale system is as follows:

$$\dot{x}(t) = Ax(t) + Bu(t) + Ev(t), \tag{1}$$
$$w(t) = Fx(t),\ v(t) = Hw(t),\ y(t) = Cx(t), \tag{2}$$

where $x, u, y, v,$ and w are, respectively, state, control, measurement output, interaction input and interaction output vectors. It is represented by a block diagonal system formed by the member subsystems (i.e. A, B, E, F, C are diagonal matrices) and the interconnection process modeled by H. H is the global coupling matrix. It contains the information of interconnections between subsystems. The elements of H is either 1 or 0 only.

$$\dot{x}(t) = \begin{bmatrix} A_1 \\ & A_2 \\ & & A_3 \end{bmatrix} x(t) + \begin{bmatrix} B_1 \\ & B_2 \\ & & B_3 \end{bmatrix} u(t) + \begin{bmatrix} E_1 \\ & E_2 \\ & & E_3 \end{bmatrix} v(t), \tag{3}$$

$$w(t) = \begin{bmatrix} F_1 \\ & F_2 \\ & & F_3 \end{bmatrix} x(t), \qquad v(t) = Hw(t). \tag{4}$$

The block diagram representing the interaction-oriented model of interconnected systems [9] is shown in Figure 3 below. This type of model can also be called two port state space model in the control literature.

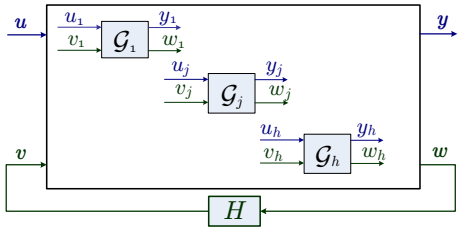

Fig. 3. Block diagram of the large-scale system Σ with h subsystems $\mathcal{G}_j$ and the interconnection process H.

2) First-Principle Equations: The differential equations for the three tanks in this washing circuit are as follows:

$$\begin{aligned}
Tank\ 1: \quad & \frac{dh_{u_1}}{dt} = -q_{u_1} + q_{feed} - a_{11}\ \rho_{feed}\ h_{u_1} \\
& \frac{dh_{o_1}}{dt} = -q_{o_1} + q_{o_2} + a_{12}\ \rho_{feed}\ h_{u_1} \\
& \frac{d\rho_{u_1}}{dt} = a_{13}\ \rho_{sl_1} + f_{add_1} + a_{14}\ h_{u_1} \\
Tank\ 2: \quad & \frac{dh_{u_2}}{dt} = -q_{u_2} + q_{feed} - a_{22}\ \rho_{feed}\ h_{u_2} \\
& \frac{dh_{o_2}}{dt} = -q_{o_2} + q_{o_2} + a_{22}\ \rho_{feed}\ h_{u_2} \\
& \frac{d\rho_{u_2}}{dt} = a_{23}\ \rho_{sl_2} + f_{add_2} + a_{24}\ h_{u_2} \\
Tank\ 3: \quad & \frac{dh_{u_3}}{dt} = -q_{u_3} + q_{feed} - a_{33}\ \rho_{feed}\ h_{u_3} \\
& \frac{dh_{o_3}}{dt} = -q_{o_3} + q_{o_2} + a_{32}\ \rho_{feed}\ h_{u_3} \\
& \frac{d\rho_{u_3}}{dt} = a_{33}\ \rho_{sl_3} + f_{add_3} + a_{34}\ h_{u_3},
\end{aligned}$$

where

h_{u_i}	is the underflow solid level in Tank i (m).
h_{o_i}	is the overflow liquor level in Tank i (m).
q_{u_i}	is the underflow flow-rate of Tank i (m^3/hrs).
q_{o_i}	is the overflow flow-rate of Tank i (m^3/hrs).
f_{add_i}	is the flocculant flow-rate of Tank i (mm^3/hrs).
ρ_{u_i}	is the underflow solid density of Tank i ($\mathrm{kg/m}^3$).
ρ_{sl_i}	is the solid density inside Tank i ($\mathrm{kg/m}^3$).
ρ_{feed}	is the slurry feed density ($\mathrm{kg/m}^3$).

$a_{i1}, a_{i2}, a_{i3}, a_{i4}$ are the process parameters of Tank i.

When the underflow pumps (regulating q_{u_i}) and overflow pumps (regulating q_{o_i}) are set in a cascade configuration, wherein their set points are obtained from the corresponding level measurements of the same tanks, the models become

$$\begin{aligned}
\frac{dh_{u_1}}{dt} &= -b_{11}h_{u_1} + q_{feed} - a_{11}\ \rho_{feed}h_{u_1} - c_{11}b_{22}h_{o_2} \\
\frac{dh_{o_1}}{dt} &= -b_{12}\ h_{o_1} + b_{22}\ h_{o_2} + a_{12}\ \rho_{feed}\ h_{u_1} \\
\frac{d\rho_{u_1}}{dt} &= a_{13}\ \rho_{sl_1} + f_{add_1} + a_{14}\ h_{u_1} \\
\frac{dh_{u_2}}{dt} &= -b_{22}h_{u_2} + q_{feed} - a_{22}\rho_{feed}h_{u_2} - c_{22}b_{22}h_{o_2} \\
\frac{dh_{o_2}}{dt} &= -b_{22}h_{o_2} + b_{22}h_{o_2} + a_{22}\rho_{feed}h_{u_2} \\
\frac{d\rho_{u_2}}{dt} &= a_{23}\rho_{sl_2} + f_{add_2} + a_{24}h_{u_2} \\
\frac{dh_{u_3}}{dt} &= -b_{33}h_{u_3} + q_{feed} - a_{33}\rho_{feed}h_{u_3} - c_{33}q_{cond} \\
\frac{dh_{o_3}}{dt} &= -b_{32}h_{o_3} + q_{cond} + a_{32}\rho_{feed}\ h_{u_3} \\
\frac{d\rho_{u_3}}{dt} &= a_{33}\rho_{sl_3} + f_{add_3} + a_{34}\ h_{u_3}
\end{aligned}$$

where b_{i1} and b_{i2} represent the set-point ratio transferred from the outer controller to the inner controller of the cascade level control loop in Tank i, while q_{cond} is the condensate flow rate feeding to the final washing stage in Tank 3.

The following linearised state-space realisation matrices (at the nominal operating point of $\rho_{u_{1o}}, \rho_{u_{2o}}, \rho_{u_{3o}}$) are then obtained:

$$A_1 = \begin{bmatrix} -b_{11} - a_{11}\rho_{u_{1o}} & 0 & 0 \\ a_{12}\rho_{u_{1o}} & -b_{12} & c_{22} \\ -a_{14} & 0 & 0 \end{bmatrix}, B_1 = \begin{bmatrix} 1 & 0 \\ 0 & 0 \\ 0 & 1 \end{bmatrix},$$

$$A_2 = \begin{bmatrix} -b_{21} - a_{21}\rho_{u_{2o}} & 0 & 0 \\ a_{32}\rho_{u_{2o}} & -b_{22} & 0 \\ -a_{24} & 0 & c_{32} \end{bmatrix}, B_2 = \begin{bmatrix} 0 \\ 0 \\ 1 \end{bmatrix},$$

$$A_3 = \begin{bmatrix} -b_{31} - a_{31}\rho_{u_{3o}} & 0 & c_{23} \\ a_{32}\rho_{u_{3o}} & -b_{32} & 0 \\ -a_{34} & 0 & 0 \end{bmatrix}, B_3 = \begin{bmatrix} -c_{31} & 0 \\ 1 & 0 \\ 0 & 1 \end{bmatrix},$$

$$F_1 = \begin{bmatrix} b_{11} & 0 & 0 \\ 0 & 0 & 1 \end{bmatrix}, F_2 = \begin{bmatrix} b_{21} & 0 & 0 \\ 0 & 0 & b_{22} \end{bmatrix},$$

$$F_3 = \begin{bmatrix} 0 & b_{32} & 0 \end{bmatrix}.$$

With the parameters provided from an actual alumina refinery project, the state space realisation matrices are provided in the following:

$$A_1 = \begin{bmatrix} -29 & 0 & 0 \\ 17 & -6 & 0.5 \\ -8 & 0 & 0 \end{bmatrix}, \quad B_1 = \begin{bmatrix} 1 & 0 \\ 0 & 0 \\ 0 & 1 \end{bmatrix},$$

$$E_1 = \begin{bmatrix} 0 & -0.4 \\ 0 & 2 \\ 0 & 0 \end{bmatrix}, \quad C_1 = \begin{bmatrix} 1 & 0 & 0 \\ 0 & 1 & 0 \end{bmatrix},$$

$$A_2 = \begin{bmatrix} -14 & 0 & 0 \\ 18 & -0.5 & 0 \\ -3 & 0 & 0.2 \end{bmatrix}, \quad B_2 = \begin{bmatrix} 0 \\ 0 \\ 1 \end{bmatrix},$$

$$E_2 = \begin{bmatrix} 2 & 0 & -1 & 0 \\ 0 & 0 & 0 & 0 \\ 0 & 0.8 & 0 & 0 \end{bmatrix}, \quad C_2 = \begin{bmatrix} 1 & 0 & 0 \\ 0 & 1 & 0 \end{bmatrix},$$

$$A_3 = \begin{bmatrix} -16 & 0 & 1 \\ 12 & -0.7 & 0 \\ -6 & 0 & 0 \end{bmatrix}, \quad B_3 = \begin{bmatrix} -0.1 & 0 \\ 1 & 0 \\ 0 & 1 \end{bmatrix},$$

$$E_3 = \begin{bmatrix} 2 \\ 0.8 \\ 0 \end{bmatrix}, \quad C_3 = \begin{bmatrix} 1 & 0 & 0 \\ 0 & 1 & 0 \end{bmatrix},$$

$$F_1 = \begin{bmatrix} 0.5 & 0 & 0 \\ 0 & 0 & 1 \end{bmatrix}, \quad F_2 = \begin{bmatrix} 0.5 & 0 & 0 \\ 0 & 0 & 1 \end{bmatrix}, \quad F_3 = \begin{bmatrix} 0 & 0.7 & 0 \end{bmatrix},$$

$$H = \left[\begin{array}{cc|cc|c} 0 & 0 & 1 & 0 & 0 \\ 0 & 0 & 0 & 1 & 0 \\ \hline 1 & 0 & 0 & 0 & 1 \\ 0 & 1 & 0 & 0 & 0 \\ \hline 0 & 0 & 1 & 0 & 0 \\ 0 & 0 & 0 & 1 & 0 \end{array}\right].$$

We have applied the technique of defining boundaries for sub-processes for lumped parameter models to the tank models here; see, e.g. [10]. This model has been used for feedback control designs in our previous work; see, e.g. [11], [12], [13], [14], [15].

III. The Predesilication Unit Operation

In the predesilication department, the extracted bauxite ores are fed into grinding machines, then preheated and circulated through a system of settling and predesilicating tanks before being mixed with heated soda in the digesters. If the process is designed with only one mill grinder, it is divided into three subsystems. The process diagram is given in Figure 4. The mill grinding area (subsystem 1) has one grinding mill (ML-1) built with a belt weigher (W-11), a mill slurry tank (T-11), and a relay tank (T-21). Each mill is installed with an independent inching control system. The heating and predesilication area (subsystem 2) has one steam heater (H-21) built with mill slurry pumps (P-21), booster pumps (P-22) and three predesilicating tanks (T-21, -22, -23) built with transfer and recirculation pumps (P-23, -24, -25).

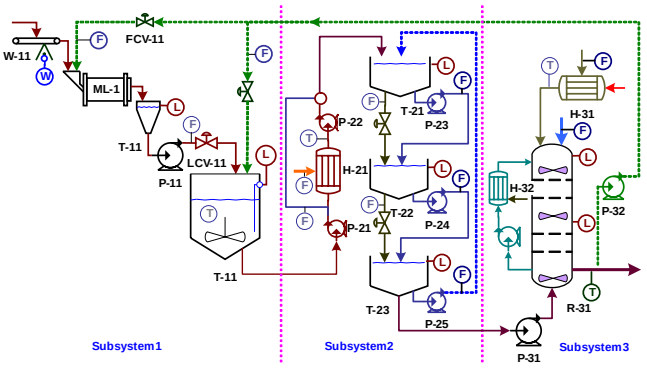

Fig. 4. Pre-desilication unit operation without parallel subsystems.

The saturated liquor from the reactor tank R-31 in subsystem 3 is extracted and recirculated back to the mill grinding area.

The large-scale system is modeled as three subsystems interconnected to each other. The control input subsystem 1 is the mill feed solid flow rate via the belt weigher (W-11). The control for this subsystem (only) is preferable with on/off (bang-bang) control. The levels in the mill, slurry and relay tanks are its states. The control inputs for the predesilication tanks in subsystem 2 are the transfer and recirculation flow rates (P-23, -24, -25). The levels in three predesilication tanks are its states. The temperature and flow control loops in this subsystem are not included in this scheme. The two control inputs of subsystem 3 are steam and caustic soda flow rates feeding to the top of the reactor tank R-31. The level and temperature in the reactor R-31 are its states.

Similarly to the counter-current washing circuit model above, the state space model of the large-scale system is as follows:

$$\dot{x}(t) = Ax(t) + Bu(t) + Ev(t), \tag{5}$$

$$w(t) = Fx(t),\ v(t) = Hw(t),\ y(t) = Cu(t), \tag{6}$$

where $x, u, y, v,$ and w are, respectively, state, control, measurement output, interaction input and interaction output vectors. It is represented by a block diagonal system formed by the member subsystems (i.e. A, B, E, F, C are block diagonal matrices) and the interconnection process modeled by H. H is the global coupling matrix. It contains the information of interconnections between subsystems. The elements of H is either 1 or 0 only.

$$A_1 = \begin{bmatrix} -1.4 & 0.3 & 0 \\ 0 & -1.8 & 1.5 \\ 0.1 & -2.7 & 1.06 \end{bmatrix}, B_1 = \begin{bmatrix} 0 \\ 0 \\ 1 \end{bmatrix},$$

$$E_1 = \begin{bmatrix} 0.58 \\ 0 \\ 0.58 \end{bmatrix}, C_1 \begin{bmatrix} 1 & 0 & 0 \\ 0 & 1 & 0 \end{bmatrix}, F_1 = \begin{bmatrix} 1 & 0 & 0 \end{bmatrix},$$

$$A_2 = \begin{bmatrix} -0.76 & 0 & 0.25 \\ .48 & -0.56 & 0 \\ 0 & 0.2 & -0.34 \end{bmatrix}, B_2 = -\begin{bmatrix} 1 & 0 & 0 \\ 0 & 1 & 0 \\ 0 & 0 & 1 \end{bmatrix},$$

$$E_2 = \begin{bmatrix} 0.8 \\ 0 \\ 0 \end{bmatrix}, C_2 = \begin{bmatrix} 1 & 0 & 0 \\ 0 & 1 & 0 \end{bmatrix}, F_2 = \begin{bmatrix} 0 & 0 & 1 \end{bmatrix},$$

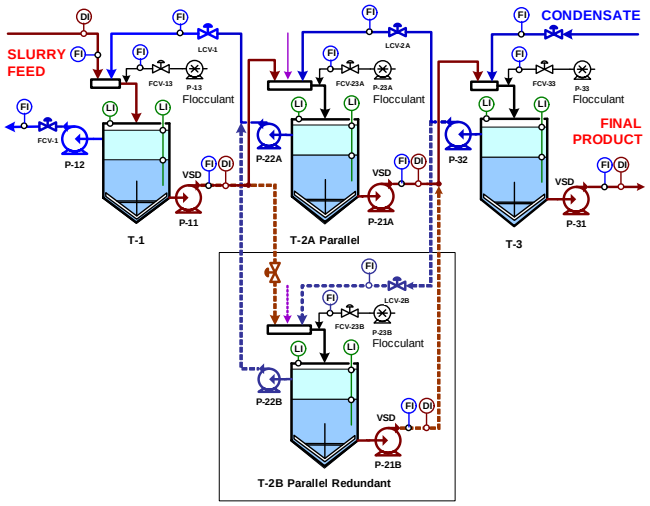

Fig. 5. Counter-current washing circuit with parallelized subsystems.

$$A_3 = \begin{bmatrix} -4.3 & 5.9 \\ -1.8 & 2.7 \end{bmatrix}, B_3 = \begin{bmatrix} 1 & 0 \\ 0 & 1 \end{bmatrix},$$

$$E_3 = \begin{bmatrix} 0.5 \\ 0 \end{bmatrix}, C_3 = \begin{bmatrix} 1 & 0 \\ 0 & 1 \end{bmatrix}, F_3 = \begin{bmatrix} 0 & 1 & 0 \end{bmatrix}, \; H = \begin{bmatrix} 0 & 0 & 1 \\ 1 & 0 & 0 \\ 0 & 0 & 0 \end{bmatrix}.$$

IV. Modeling of Parallelized Process Streams

In order for the mineral processing plants to operate continuously while doing equipment maintenances, it is usually designed to have backing up streams of process systems or unit operations within every department. We called this backing up stream as parallelized, or parallel splitting streams, or parallel redundant, in the state space model. The parallelized term is used to distinguish with the parallel subsystems [16] formally defined in the control literature for non-splitting streams.

A. Parallelized Subsystems

The process diagram of the washing circuit with the parallel redundant washing stage T-2b is given in Figure 5. The nested system models, consisting of Units and Subsystems, will be deployed for the large-scale system having mixed connection configurations like this one. The large-scale process is grouped into three Units. Unit 1 has two Subsystems. Units 2 an 3 each has one Subsystem.

For clarity, the modeling process for generic cases is given in detail here. the A large-scale system is viewed as consisting of two layers, Units and Subsystems. Consider a large-scale system Σ consisting of h units, denoted as $\mathcal{G}_j, j = 1 \dots h$. Each unit $\mathcal{G}_j$ has g_j subsystems, denoted as $\mathcal{S}_{ji}, i = 1 \dots g_j$. The hierarchical tree representing the nested subsystems is given in Figure 6 to illustrate subsystem denotations in this chapter and Thesis. Each subsystem $\mathcal{S}_{ji}$ is represented by the discrete-time state space model of the form

$$\mathcal{S}_{ji}: \begin{cases} x_{ji}(k+1) = A_{ji}\, x_{ji}(k) + B_{ji}\, u_{ji}(k) + E_{ji}\, v_{ji}(k), \\ y_{ji}(k) = C_{ji}\, x_{ji}(k), \quad w_{ji}(k) = F_{ji}\, x_{ji}(k), \end{cases} \tag{7}$$

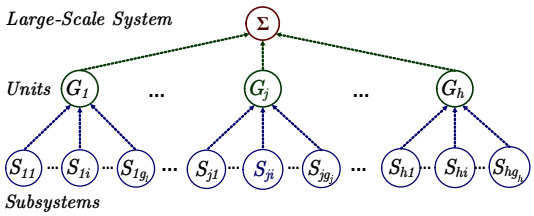

Fig. 6. Denotations for Subsystems, Units and the Large-Scale System.

where $E_{ji} = [E_{\pi ji}\ E_{\sigma ji}]$, $v_{ji}^T = [v_{\pi ji}^T\ v_{\sigma ji}^T]$, $F_{ji} = [F_{\pi ji}\ F_{\sigma ji}]$, $w_{ji}^T = [w_{\pi ji}^T\ w_{\sigma ji}^T]$, in which $v_{\sigma ji}$ and $w_{\sigma ji}$ are *serial coupling* input and output vectors respectively, while $v_{\pi ji}$ and $w_{\pi ji}$ are *parallelized coupling* input and output vectors; x_{ji} is the state vector, y_{ji} is the measurement output vector, u_{ji} is the control input vector. It is notably that, there are $h_\Sigma := \sum_{j=1}^{h} g_j$ subsystems $\mathcal{S}_{ji}$ in Σ.

1) Serial Connections: : Two subsystems $\mathcal{S}_{\xi\mathsf{i}}$ and $\mathcal{S}_{\zeta\mathsf{o}}$ are said to be *serially connected* (SC) if the coupling input vector $v_{\sigma\xi\mathsf{i}}$ of $\mathcal{S}_{\xi\mathsf{i}}$ is the coupling output vector $w_{\sigma\zeta\mathsf{o}}$ of $\mathcal{S}_{\zeta\mathsf{o}}$, i.e.

$$(\mathrm{SC})\ v_{\sigma\xi\mathsf{i}}(k) = w_{\sigma\zeta\mathsf{o}}(k). \tag{8}$$

In the following, M_j (of unit $\mathcal{G}_j$) denotes the diagonal matrix $\mathrm{diag}[M_{ji}]_1^{g_j}$, and v_{*j} denotes the stacking vector $[{v_{*j1}}^T \dots {v_{*jg_j}}^T]^T$ (i.e. unit subscript j remains). A unit $\mathcal{G}_j$ is represented by the block diagonal system formed by g_j parallelized subsystems $\mathcal{S}_{ji}$ as

$$\mathcal{G}_j: \begin{cases} x_j(k+1) = A_j\, x_j(k) + B_j\, u_j(k) + E_j\, v_j(k), \\ y_j(k) = C_j\, x_j(k), \quad w_j(k) = F_j\, x_j(k), \end{cases} \tag{9}$$

where $E_j = [E_{\pi j}\ E_{\sigma j}]$, $v_j^T = [v_{\pi j}^T\ v_{\sigma j}^T]$, $F_j = [F_{\pi j}\ F_{\sigma j}]$, $w_j^T = [w_{\pi j}^T\ w_{\sigma j}^T]$.

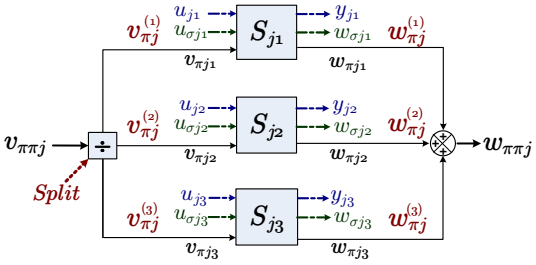

Fig. 7. Parallel Connections of a Unit $\mathcal{G}_j$ having Three Subsystems.

2) Parallel Connections within One Unit: : The parallelized coupling vectors $v_{\pi ji}$ and $w_{\pi ji}$ of all subsystems $\mathcal{S}_{ji}$ belonging to a unit $\mathcal{G}_j$ are assumed, without loss of generality, having the same size. If there is only one parallelized signal, the block diagram of the parallelized connections within a unit $\mathcal{G}_j$ having three subsystems ($g_j = 3$) is given in Figure 7. The divider operator at $v_{\pi\pi j}$ in this figure represents the splitting of $v_{\pi\pi j}$ into $v_{\pi j}^{(\ell)}$.

Two new signals, $v_{\pi\pi j}$ and $w_{\pi\pi j}$ are introduced here. While the outputs $w_{\pi j}$ are sum up to become $w_{\pi\pi j}$, the input

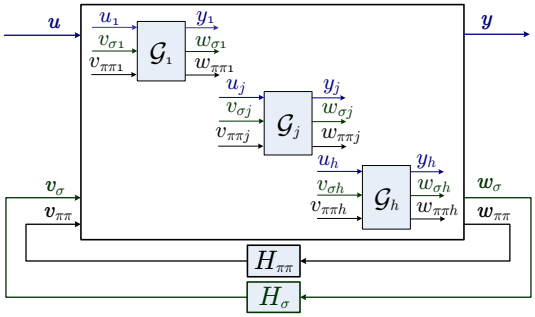

Fig. 8. Block Diagram of the Large-Scale System Σ with Units $\mathcal{G}_j$.

$v_{\pi\pi j}$ is split up into $v_{\pi j}$. Their relationships are represented by two matrices Ψ_{v_j} and Ψ_{w_j}, which are defined as

$$\text{(PC)} \quad \begin{aligned} v_{\pi\pi j} &= v_{\pi j1} + \cdots + v_{\pi j g_j} := \Psi_{v_j} v_{\pi j}, \\ w_{\pi\pi j} &= w_{\pi j1} + \cdots + w_{\pi j g_j} := \Psi_{w_j} w_{\pi j}, \end{aligned} \tag{10}$$

where $v_{\pi j}^T = [v_{\pi j1}^T \dots v_{\pi j g_j}^T], w_{\pi j}^T = [w_{\pi j1}^T \dots w_{\pi j g_j}^T]$.

In the parallel redundant configuration, where the material or energy flows are split into smaller flows to each subsystems, it is impossible to have a constant splitting ratio at all time, but rather dynamic ratios. The splitting ratios between $v_{\pi ji}$ of $v_{\pi j}$ should, therefore, be *time-varying* and *unknown*. Due to these unknown splitting ratios of parallelized subsystems, the connectivity of the large-scale interconnection process can not be established on the basis of subsystems. The common input and output vectors, $v_{\pi\pi j}$ and $w_{\pi\pi j}$, of parallelized connections are involved in the connection processes, instead of $v_{\pi j}$ and $w_{\pi j}$ of subsystems.

In the following, M (of Σ) denotes the block diagonal matrix $\text{diag}[M_j]_1^h$, and v_* denotes the stacking vector $[{v_*1}^T \dots {v_*h}^T]^T$ (unit subscripts j vanish). The large-scale system Σ is represented by the block diagonal system formed by h diagonal units $\mathcal{G}_j$ (or h_Σ subsystems $\mathcal{S}_{ji}$), and the large-scale interconnection processes $H_\sigma, H_{\pi\pi}$ as

$$\Sigma : \begin{cases} x(k+1) = A\,x(k) + B\,u(k) + Ev(k) \\ y(k) = Cx(k),\ w(k) = Fx(k), \\ v_{\pi\pi}(k) = H_{\pi\pi}\, w_{\pi\pi}(k),\ v_\sigma(k) = H_\sigma\, w_\sigma(k). \end{cases} \tag{11}$$

where
$E = [E_\pi\ E_\sigma], F = [F_\pi\ F_\sigma], v^T = [v_\pi^T\ v_\sigma^T], w^T = [w_\pi^T\ w_\sigma^T]$.

The parallelized connection process inside Σ is as follows:

$$v_{\pi\pi}(k) = \Psi_v\, v_\pi(k),\ w_{\pi\pi}(k) = H_{\pi\pi}\Psi_w\, w_\pi(k), \tag{12}$$

where $\Psi_v = \text{diag}[\Psi_{v_j}]_1^h$, $\Psi_w = \text{diag}[\Psi_{w_j}]_1^h$.

The interconnections between units and subsystems are specified by the interconnection matrices $H_{\pi\pi}$ and H_σ respectively. The elements of $H_{\pi\pi}$ and H_σ are zero or one only. The block diagrams of the large-scale system Σ from the unit perspective are depicted in Figure 8.

V. Conclusion

Developing state space models for the two mineral separation processes for the multi-variable feedback control design purpose has been presented. By employing the interaction-oriented model of interconnected systems introduced in the control literature, the complex process systems have been modeled by the granularity of its subsystems and their interactions. The first-principle differential equations describing the corresponding process systems have been used. The linearised state realisation matrices are then obtained from the differential equations as a direct result. The developed models have been successfully deployed with decentralised and distributed model predictive control schemes in previous work.

References

[1] Hoffman T and H. P. Hutchinson, "The simulation of the Bayer process for extracting alumina from bauxite ore," *Proceedings of Symposium on Computer Design and Erection of Chemical Plants,* Czechoslovakia, pp. 451–485, 1975.

[2] Leslie R. A. and J. R. Blair, "The dynamic modelling of caustic concentration in the Bayer process," *Proceedings of APCOM Symposium 5*, pp. 137–14, 1975.

[3] Sidrak Y. L., "Dynamic simulation and control of the Bayer process - A Review," *Industrial and Engineering Chemistry Research*, vol. 40, pp. 1146–1156, 2001.

[4] Hodouin D, S. L. Jämsä-Jounela, M. T. Carvalhoc, and L. Bergh, "State of the art and challenges in mineral processing control," *Control Engineering Practice*, vol. 9, no. 1, pp. 995–1005, 2001.

[5] Ouellet V., S. Bergeron, and D. Verville, "Bayer process control at Alcan Vaudreuil works," *Proceedings of 12th IFAC Symposium on Automation in Mining, Mineral and Metal Processing*, vol. 12, no. 1, p. Quebec, 2007.

[6] Liu J., W. Li, Y. Wang, and Z. Liu, "Model on batch seeded gibbsite precipitation from Bayer liquor," *Proceedings of TMS Annual Meeting - Light Metals 2009*, pp. San Francisco, 207–211, 2009.

[7] Harder J., "Trends in the extraction of bauxite and alumina," *Aufbereitungs-Technik/Mineral Processing*, vol. 51, no. 5, pp. 44–57, 2010.

[8] Henrickson L., "The need for energy efficiency in Bayer refining," *Proceedings of TMS Annual Meeting - Light Metals'10,* Seattle, pp. 173–178, 2010.

[9] Lunze J., *Feedback Control of Large Scale Systems*. Prentice Hall, 1992.

[10] Hangos K. M. and I. T. Cameron, *Process Modelling and Model Analysis*. Academic Process, 2001.

[11] Tri Tran, H. D. Tuan, Q. P. Ha, and Hung T. Nguyen, "Toward plant-wide control of reticulated systems arising in alumina refineries with online stabilisation," *Proceedings of the 18th IFAC World Congress,* Milano, Italy, August 2011, pp. 10529–10534, 2011.

[12] Tri Tran, H. D. Tuan, Q. P. Ha, and Hung T. Nguyen, "Stabilising agent design for the control of interconnected systems," *International Journal of Control*, vol. 84, pp. 1140–1156, July 2011.

[13] Tri Tran, Q. P. Ha, and Hung T. Nguyen, "Semi-automatic control of modular systems with intermittent data losses," *Proceedings of the 7th IEEE Conference on Automation Science and Engineering* CASE'11, pp. 625–630, Trieste, Italy, August 2011.

[14] Tri Tran and Q. P. Ha, "Set-point tracking semi-automatic control of interconnected systems with local input disturbances," *Proceedings of the 1st Australian Control Conference AUCC'11,* Melbourne, Australia, pp. 224–229, Nov. 2011.

[15] Tri Tran, H. D. Tuan, Q. P. Ha, and H. T. Nguyen, "Decentralised model predictive control of time-varying splitting parallel systems," in *Control of Linear Parameter Varying Systems with Applications* (M. Javad and C. Scherer, eds.), pp. 217–251, Springer-Verlag, 2012.

[16] B. Brogliato, R. Lozano, B. Maschke, and O. Egeland, *Dissipative Systems Analysis and Control: Theory and Apps.* Springer, 2006.